

A unified framework for equation discovery and dynamic prediction of hysteretic systems

Siyuan Yang^a, Wei Liu^{a,b}, Zhilu Lai^{a,c,*}

^a*Internet of Things Thrust, The Hong Kong University of Science and Technology (Guangzhou), China*

^b*Department of Industrial Systems Engineering and Management, National University of Singapore, Singapore*

^c*Department of Civil and Environmental Engineering, The Hong Kong University of Science and Technology, China*

Abstract

Hysteresis is a nonlinear phenomenon with memory effects, where a system's output depends on both its current state and past states. It is prevalent in various physical and mechanical systems, such as yielding structures under seismic excitation, ferromagnetic materials, and piezoelectric actuators. Analytical models like the Bouc-Wen model are often employed but rely on idealized assumptions and careful parameter calibration, limiting their applicability to diverse or mechanism-unknown behaviors. Existing equation discovery approaches for hysteresis are often system-specific or rely on predefined model libraries, which limit their flexibility and ability to capture the hidden mechanisms. To address these, this research develops a unified framework that integrates learning of internal variables (commonly used in modeling hysteresis) and symbolic regression to automatically extract internal hysteretic variable, and discover explicit governing equations directly from data without predefined libraries as required by methods such as sparse identification of nonlinear dynamics (SINDy). Solving the discovered equations naturally enables prediction of the dynamic responses of hysteretic systems. This work provides a systematic view and approach for both equation discovery and characterization of hysteretic dynamics, defining a unified framework for these types of problems.

*Corresponding author.

Email addresses: syang724@connect.hkust-gz.edu.cn (Siyuan Yang), weiliu@u.nus.edu (Wei Liu), zhilulai@ust.hk (Zhilu Lai)

Keywords: Hysteretic dynamic systems; equation discovery; symbolic regression; internal variable learning

1. Introduction

Hysteresis is a common nonlinear phenomenon observed in a broad spectrum of engineering and physical systems, including ferromagnetic materials [1], piezoelectric actuators [2], structural materials [3], damping devices [4, 5], and shape memory alloys [6]. Hysteresis, characterized by its path-dependent behavior, refers to systems in which the output depends not only on the current state, but also on the history of past states. This memory effect often appears as input-output loops, and is especially evident in systems that involve energy dissipation, plastic deformation, or phase transitions [7, 8]. In nonlinear dynamic systems, hysteresis presents significant challenges for modeling, control, and prediction, owing to its multivalued behavior, rate dependence, and sensitivity to input history. Accurately capturing hysteresis behavior is therefore crucial in applications such as structural health monitoring [9], smart material design [10], and precision actuation systems [11, 12].

In response to these needs, numerous mathematical models have been proposed over the past decades to characterize hysteretic behaviors. Among these, the Bouc-Wen model [7] is one of the most widely adopted, owing to its capability to replicate a wide variety of hysteresis loops via differential equations that describe the evolution of an internal variable. Its parameters provide physical interpretability and offer flexibility in capturing both softening and hardening behaviors. In addition to the Bouc-Wen model, other approaches such as the Preisach [13], Duhem [14], and Prandtl-Ishlinskii [15] models offer complementary frameworks, and have been effectively applied in domains where rate-independent behavior or saturation effects are predominant. However, these models typically require prior knowledge of the system structure or involve challenging calibration procedures, limiting their generalizability to complex or mechanism-unknown hysteretic dynamics.

In recent years, data-driven modeling has opened new venues for discovering governing laws directly from measured data [16–21]. The sparse identification of nonlinear dynamics (SINDy) [22] has shown strong potential in extracting compact and interpretable dynamic equations, by applying sparse regression with a predefined library of candidate functions. Extensions such as SINDy with control [22], physics-informed SINDy [23, 24], implicit

SINDy [25], and a sparse structural system identification method applied to hysteretic systems [26] have significantly expanded its applicability to control systems, hidden-variable models, constrained physical systems, and hysteretic dynamics (our focus in this paper). Nevertheless, the effectiveness of SINDy-type methods strongly relies on the expressiveness of the chosen function library, which constrains their ability to capture non-polynomial dynamics, rate-dependent behaviors, and discontinuities. Selecting an appropriate function library is itself a nontrivial task, often requiring prior knowledge or trial-and-error tuning. Furthermore, many dynamical systems involve essential internal states—referred to as *internal hysteretic variables* in hysteretic systems, or simply as *internal variables* for brevity in this paper – which are not directly observable but are required to capture implicit evolution and memory effects. Consequently, these methods are not well-suited for such cases.

These limitations become particularly critical in the context of hysteretic systems, where complex memory-dependent behaviors introduce additional challenges. (i) First, internal variables – such as restoring forces or internal displacements – are often not directly measurable [27], complicating the construction of state-space representations. (ii) Second, hysteresis is typically characterized by strong memory and rate dependence, which static or memoryless models are unable to capture. In this research, the proposed framework addresses these issues through a proposed solver-based internal variable learning scheme, which enables the learning of hysteretic variables (see Section 3.2 for details). (iii) Third, the presence of non-smooth mathematical operations, such as absolute values or sign functions, precludes the use of Taylor expansions and hinders the application of gradient-based optimization techniques. Our framework further tackles this challenge by employing equation discovery to flexibly utilize data for recovering explicit expressions of complex structures (see Section 3.3 for details). These challenges become even more pronounced in dynamic systems where the governing laws are implicit or nonlinear in unstructured ways. Consequently, there is a growing need for modeling frameworks capable of simultaneously inferring internal variables, capturing memory effects, and producing interpretable governing equations directly from data.

A variety of approaches have been proposed for equation discovery in hysteretic systems, which in this paper are classified according to the extent of prior knowledge assumed about the governing equations. In Figure 1, we organize the literature into four categories based on whether the struc-

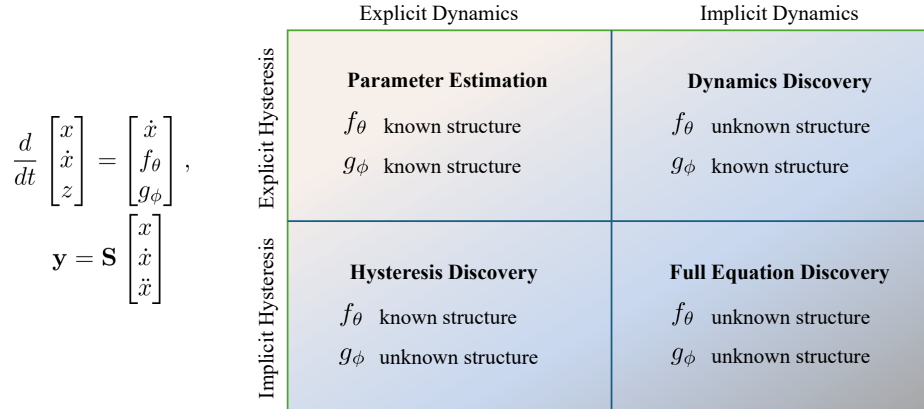


Figure 1: Classification of equation discovery approaches for hysteretic systems according to the assumed knowledge of the primary dynamics motion equation (f_θ) and the hysteretic link equation (g_ϕ). The state variables $x, \dot{x}, \ddot{x}, z \in \mathbb{R}^1$ denote the scalar displacement, velocity, acceleration, and internal hysteretic variable, respectively. $\mathbf{y} \in \mathbb{R}^d$ denotes the available measurements with selection matrix \mathbf{S} specifying the observed quantities. All these variables are dependent on t , which is omitted here for brevity. Each quadrant represents a level of prior structural specification.

ture of the primary dynamics equation (f_θ) and the hysteretic link equation (g_ϕ) are explicitly known or unknown. In the majority of existing studies [26, 28], structural dynamics is assumed to follow an explicit linear form or other types of known forms, while the hysteretic component is represented by an additional differential equation whose functional forms are to be discovered. Under this setting, the equation discovery task is reduced to symbolically identifying the hysteretic link equation (*Hysteresis Discovery* quadrant) [29, 30] or estimating parameters when structures of both equations are known (*Parameter Estimation* quadrant) [31–33]. Such assumptions greatly simplify the problem but restrict applicability to systems where the underlying structural model is already well characterized. In contrast, frameworks that assume unknown (implicit) structures in the primary dynamics equation (*Dynamics Discovery* quadrant) are far less common, particularly when hysteretic effects are present. When both the structural dynamics and the hysteretic link equations are unknown (*Full Equation Discovery* quadrant), the problem becomes substantially more challenging, requiring the simultaneous inference of two coupled, potentially nonlinear and memory-dependent governing equations. To the best of our knowledge, no prior work has demon-

strated a fully symbolic equation discovery framework capable of addressing this most general setting. This highlights the need for a unified approach that can infer both structural and hysteretic dynamics directly from data, without relying on predefined equation forms.

In this research, we propose a unified framework that integrates internal variable learning and symbolic regression (SR) to address the challenges of hysteretic equation discovery. The framework enables direct inference of internal hysteretic variables and recovery of explicit and interpretable governing equations without relying on predefined model libraries. Our contributions are threefold: (i) we provide a classification of equation discovery approaches for hysteretic systems and establish a unified framework that accommodates different levels of prior knowledge; (ii) we introduce a solver-based scheme that enables learning of the internal hysteretic variable and a SR strategy that discovers nonlinear and fractional hysteretic laws directly from data; (iii) we validate the framework on synthetic benchmarks, a complex structure with high-order nonlinear and fractional terms, and shake-table experiments, demonstrating superior accuracy and generalizability compared with existing methods.

The remainder of this paper is organized as follows. Section 2 provides necessary preliminaries. Section 3 introduces the proposed methodology in detail. Section 4 presents numerical and experimental validation results. Section 5 concludes the paper with a summary of findings and directions for future research.

2. Preliminaries

2.1. Hysteretic models

In modeling hysteretic systems, internal variables are commonly introduced to mathematically represent memory effects and capture nonlinear, history-dependent behavior, which allows the system’s response to account for past states.

Among hysteresis models, the Bouc-Wen model [7] is one of the most widely used, owing to its simplicity, and its capacity to represent a broad range of hysteretic responses. It provides a set of differential equations to describe the evolution of internal variables, and is capable of capturing both rate-dependent and asymmetric behaviors. The dynamics motion equation for a single degree-of-freedom (SDOF) nonlinear mass-spring-damper system

with hysteresis can be expressed as follows:

$$m\ddot{x}(t) + c\dot{x}(t) + F(t) = u(t), \quad (1)$$

where $x(t)$ is the displacement response; $u(t)$ is the external excitation; m is the mass; c is the damping coefficient; and $F(t)$ is the nonlinear restoring force that accounts for both elastic and hysteretic contributions. The restoring force is defined as:

$$F(t) = kx(t) + \alpha z(t), \quad (2)$$

where k is the stiffness, α is the hysteretic coefficient, and $z(t)$ is the internal hysteretic variable. Substituting equation Eq.(2) into Eq.(1), the equation of motion is rewritten as:

$$m\ddot{x}(t) + c\dot{x}(t) + kx(t) + \alpha z(t) = u(t). \quad (3)$$

Notably, setting $\alpha = 0$ reduces the equation to classical linear behaviors.

The evolution of the internal hysteretic variable $z(t)$ is governed by the Bouc-Wen hysteresis differential equation, which can also be written as an explicit function of $\dot{x}(t)$ and $z(t)$ for compactness and interpretability (for conciseness, we drop t in the equation):

$$\dot{z}(\dot{x}, z) = A\dot{x} - \beta|\dot{x}||z|^{n-1}z - \gamma\dot{x}|z|^n. \quad (4)$$

In this formulation, the parameter A serves as a linear amplification factor that scales the influence of the displacement rate on the evolution of the internal variable. The coefficients β and γ jointly shape the energy dissipation and curvature of the hysteresis loop, with β primarily influencing the width and dissipation of the loop, while γ controls its nonlinear curvature. In most existing research [26, 30, 34], the exponent n is typically restricted to integer values, such as $n = 1$. In this research, we generalize the formulation by allowing n to take more general, including fractional values, thereby enabling richer characterization of various hysteresis.

The variable $z(t)$, representing the internal hysteretic variable, is typically unmeasurable in practical scenarios, and must be inferred from the dynamics of the observed system. This unobservability poses significant challenges for equation discovery, and motivates the use of learning-based approaches to recover the governing evolution law of $z(t)$ from data. Traditional approaches often rely on optimization-based techniques [35, 36], which may suffer from

issues such as non-convexity and sensitivity to noise, while other methods are built upon restrictive assumptions or depend on predefined functional libraries, such as SINDy [10, 22, 37]. Moreover, regression-based formulations like SINDy typically do not impose temporal coherence across time series, which limits their ability to capture complex hysteretic behaviors. More recently, physics-guided machine learning methods have been introduced to address these limitations [38, 39], including hybrid models that integrate neural networks with the physical structure of Bouc-Wen dynamics. These approaches aim to preserve physical interpretability while harnessing the representational power of data-driven models. It is worth noting that the Bouc-Wen model here serves merely as a representative example, while the proposed framework is not restricted to this specific formulation, and can be applied to a broader class of hysteretic systems.

2.2. Solvers of dynamic system

The governing equations of nonlinear dynamic systems are rarely solvable in closed form, and thus numerical integration schemes are commonly employed to approximate their time evolution. Classical approaches include implicit and explicit methods such as the Newmark- β method, widely used in structural dynamics [40], linear multistep methods including Adams-Bashforth and Adams-Moulton schemes [41], and the family of Runge-Kutta algorithms [42]. Each solver provides a trade-off between accuracy, stability, and computational efficiency, and the choice of method is usually problem dependent.

For hysteretic models such as the Bouc-Wen formulation, the dynamics are described by a set of coupled nonlinear ordinary differential equations (ODEs) involving both the displacement response and an internal hysteretic variable. These equations can be integrated using standard time-stepping schemes, provided that sufficient resolution is maintained to capture the nonlinear hysteretic transition. In practice, explicit solvers are often favored for their simplicity and efficiency when the system stiffness is moderate.

Among these available options, the classical fourth-order Runge-Kutta (RK4) method is particularly attractive, offering a good balance between accuracy and computational cost. It is easy to implement and has been widely applied in physics and engineering for nonlinear system simulations. In this research, the RK4 scheme is embedded into the internal variable learning process to integrate the hysteretic dynamics, yielding reliable reference trajectories that facilitate subsequent equation discovery.

2.3. Symbolic regression

Symbolic regression (SR) is a data-driven modeling approach that seeks to uncover the underlying mathematical relationships governing a system by simultaneously identifying both the model structure and its parameters [43]. Unlike conventional regression methods that assume a predefined functional form and focus solely on parameter estimation, SR performs a global search over the space of possible mathematical expressions – typically represented as expression trees – to find the model that best fits the data. This search is guided by principles of accuracy, parsimony, and interpretability.

Mathematically, given a set of input-output data pairs $\{(\mathbf{x}_i, y_i)\}_{i=1}^N$, SR seeks to find an analytical function $h(\cdot) \in \mathcal{H}$ such that:

$$y_i \approx h(\mathbf{x}_i; \boldsymbol{\theta}), \quad \forall i = 1, \dots, N, \quad (5)$$

where \mathcal{H} denotes the space of candidate symbolic expressions constructed from a predefined set of mathematical operators (e.g., $+$, $-$, \times , \div , \sin , $\cos \dots$), and $\boldsymbol{\theta}$ represents any tunable parameters involved in the expression. The optimal expression h^* is typically obtained by solving:

$$h^* = \arg \min_{h \in \mathcal{H}} (\mathcal{L}(h) + \lambda \Omega(h)), \quad (6)$$

where $\mathcal{L}(h)$ is a loss function measuring the prediction error (e.g., mean squared error); $\Omega(h)$ is a complexity penalty term (e.g., number of nodes in the expression tree); and λ is a regularization coefficient controlling the trade-off between accuracy and simplicity.

A defining feature of SR is its remarkable ability to discover explicit closed-form expressions without requiring prior specification of the model structure [44]. This property is particularly desirable in scientific discovery tasks where transparency and analytical interpretability are truly essential. Unlike black-box models such as neural networks, SR yields interpretable equations that can be directly analyzed, validated, or modified by domain experts. Recent algorithmic advances, including genetic programming, Monte Carlo tree search, and hybrid gradient-evolution strategies, have substantially improved both the computational efficiency and the overall expression quality of SR-generated models. Among these, notably, PySR [43] integrates evolutionary search with just-in-time compiled operators, thereby enabling scalable and efficient exploration of large expression spaces in scientific applications. Its application within the proposed framework is described in Section 3.3.

3. Methodology

3.1. Problem definition and formulation

In this research, our objective is to output explicit differential equation representations of hysteretic systems, with both equation discovery and dynamic prediction. The proposed framework first introduces a state-space formulation (detailed in Eq.(7)), as illustrated in Figures 1 and 2, where f_θ denotes the dynamic motion equation and g_ϕ represents the hysteretic link equation. The proposed unified framework is applicable to all four cases shown in Figure 1. Here, we focus on two more complex cases in which the hysteretic link equation (g_ϕ) is unknown, namely, *Case 1: Hysteresis Discovery* and *Case 2: Full Equation Discovery*. The remaining two cases can be addressed using analogous procedures within the same framework. Accordingly, our goal is to identify the explicit expressions of both f_θ and g_ϕ .

The proposed framework then introduces a learnable hysteretic model and provides the corresponding formulations for different cases. The key distinction between *Case 1* and *Case 2* lies in whether the structure of the dynamic motion equation (f_θ) is known. For *Case 1: Hysteresis Discovery*, assuming that the dynamic motion equation is known as in Eq.(3), we can get the expression of the acceleration term \ddot{x} . That is, f_θ can be expressed with unknown parameters m, c, k, α as $f_\theta = (u - c\dot{x} - kx - \alpha z)/m$ (t is omitted for brevity). Here, it is also equivalent to f_θ where $\theta = \{m, c, k, \alpha\}$, and z is treated as a learnable parameter. For *Case 2: Full Equation Discovery*, since the structure of the dynamic motion equation is unknown, it is represented by a neural network $\mathcal{N}(\cdot)$, parameterized by learnable parameters θ , i.e., $f_\theta = \mathcal{N}(x, \dot{x}, u; \theta, z)$. Here, the internal variable z is also treated as an additional learnable parameter within the model.

In both *Case 1* and *Case 2*, the structure of the hysteretic link equation (g_ϕ) remains unknown. Therefore, the internal hysteretic variable z is regarded as a learnable parameter and jointly optimized during training. Its time derivative is computed using finite differences, denoted as $\text{Diff}(z)$. Unlike the neural network representation adopted for f_θ in *Case 2: Full Equation Discovery*, z is directly modeled as a learnable parameter rather than through another neural network. This design choice is adopted since the hysteretic link (g_ϕ) has a more complex expression that is difficult to represent accurately using a neural network, while only the value of z is required in this step. Therefore, treating z as a learnable parameter provides a more flexible and accurate formulation. Accordingly, the hysteretic link equation can

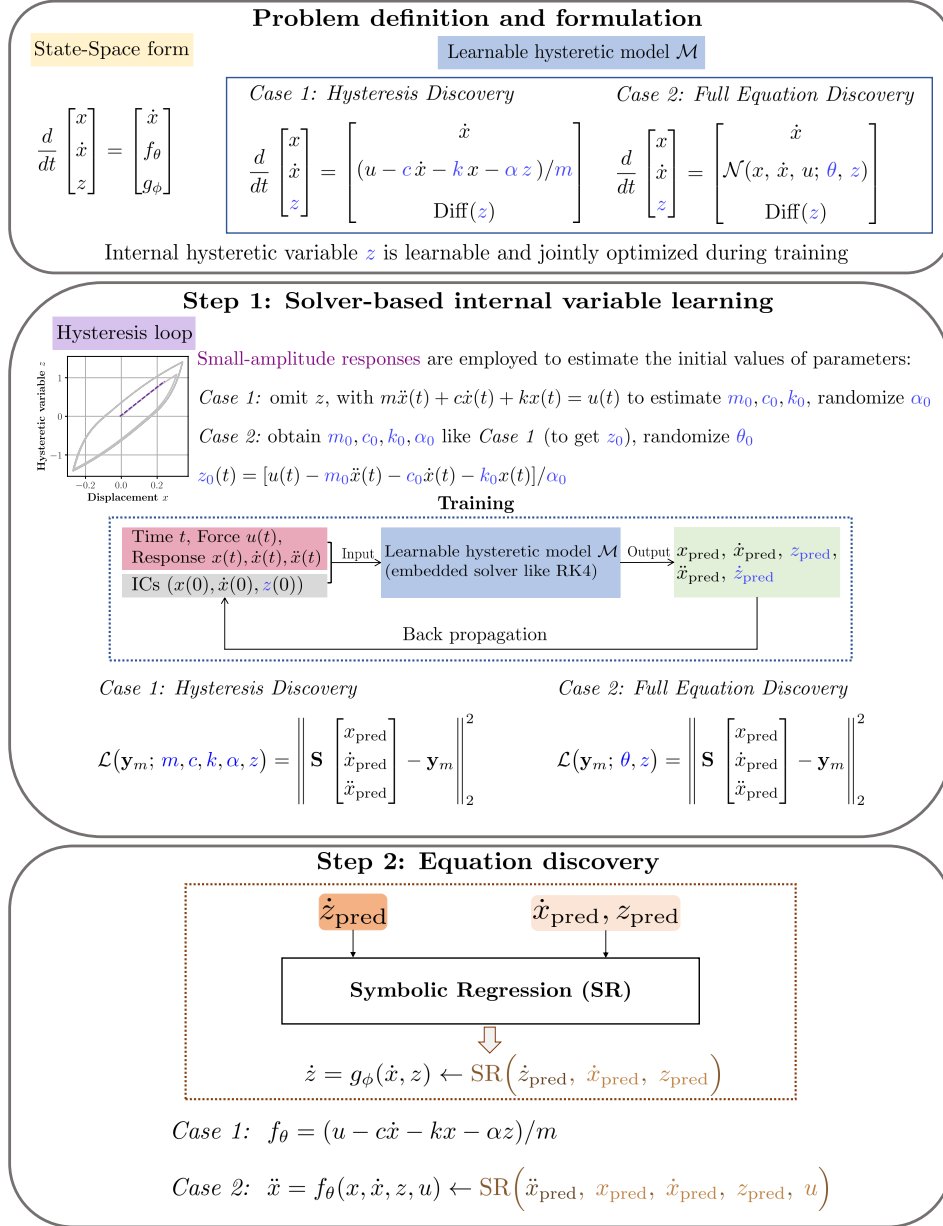


Figure 2: The proposed unified framework for equation discovery and dynamic prediction of hysteretic systems. **Problem definition and formulation:** The state-space form and learnable hysteretic model are established to describe the system dynamics. Two cases in Figure 1 are considered as typical examples, where the hysteretic link equation (g_ϕ) is unknown. The internal hysteretic variable z is treated as a learnable parameter and jointly optimized during training. Its time derivative is computed via finite differences, denoted $\text{Diff}(z)$. **Step 1:** Small-amplitude responses are employed to estimate the initial parameter values. A differentiable ODE solver is embedded to learn internal variable z and system parameters, with the selection matrix \mathbf{S} (as in Fig. 1) specifying the observed components in the loss function. **Step 2:** Symbolic regression (SR) extracts explicit and interpretable governing equations for both the dynamics motion equation (f_θ) (if *Case 2*) and hysteretic link equation (g_ϕ).

be expressed as $g_\phi = \text{Diff}(z)$, which maintains consistency with the overall problem formulation. Thus, the formulations corresponding to both cases are established. For the other two cases illustrated in Figure 1, where the hysteretic link equation is known (e.g., Eq.(4)), the same formulation strategy can be readily applied. With these formulations in place, the subsequent steps—*Solver-based internal variable learning* and *Equation discovery*—can then be performed conveniently.

3.2. Solver-based internal variable learning

The second step of the proposed framework focuses on solver-based internal variable learning, where the responses of the formulated state-space equations are simulated through an embedded numerical solver rather than by pointwise regression. Unlike pointwise regression methods that approximate the system’s temporal evolution at individual time steps, the solver-based approach enforces temporal consistency by integrating the governing equations over time, thereby capturing the implicit dependence of the internal hysteretic variable on the system states.

To initialize the model parameters, small-amplitude responses are employed to offer an estimate of the initial values of the system parameters. For *Case 1: Hysteresis Discovery*, to estimate the initial value of m, c, k , the internal variable $z(t)$ in Eq.(3) is omitted, and the dynamic motion equation $m\ddot{x}(t) + c\dot{x}(t) + kx(t) = u(t)$ is used to estimate the initial value m_0, c_0, k_0 , while the initial value α_0 is randomly initialized. For *Case 2: Full Equation Discovery*, the parameters m_0, c_0, k_0, α_0 are obtained in the same way as in *Case 1: Hysteresis Discovery* for estimating the initial value z_0 , while the neural network parameters θ_0 are randomly initialized. Based on these settings and Eq.(3), the initial value of internal hysteretic variable z_0 can be expressed as $z_0(t) = [u(t) - m_0\ddot{x}(t) - c_0\dot{x}(t) - k_0x(t)]/\alpha_0$. This procedure provides a physically consistent initialization for the learnable hysteretic model, improving convergence and stability of solver-based optimization.

In this step, the governing equations are formulated into a state-space representation, within which a learnable hysteretic model is embedded inside a differentiable ODE solver such as RK4. To make this explicit, the system can be written in the following state-space form:

$$\frac{d}{dt} \begin{bmatrix} x \\ \dot{x} \\ z \end{bmatrix} = \begin{bmatrix} \dot{x} \\ f_\theta \\ g_\phi \end{bmatrix}, \quad (7)$$

where x denotes the displacement, \dot{x} is the velocity, and z denotes the hysteretic internal variable; f_θ denotes the dynamic motion equation and g_ϕ represents the hysteretic link equation. Given the known time stamps t , the system responses such as $x(t)$, $\dot{x}(t)$, and $\ddot{x}(t)$ (any of which can be derived or integrated from the others), the external excitation $u(t)$, and the initial conditions $(x(0), \dot{x}(0), z(0))$, these quantities are fed into the learnable hysteretic model within the solver to obtain the predicted responses x_{pred} , \dot{x}_{pred} , and \ddot{x}_{pred} . As described previously, z is defined as a learnable parameter within the model. During each iteration, the errors between predicted values and desired measured data are back-propagated through the solver, to update conditions $z(0)$ and system parameters θ , allowing z_{pred} to be iteratively refined.

We design a loss function that is flexible to the types of available data. As shown in Figures 1 and 2, the formulation is flexible with respect to the available system responses, such that it can accommodate a subset of displacement, velocity, or acceleration measurements. The corresponding loss functions for the two cases are:

$$\mathcal{L}(\mathbf{y}_m; m, c, k, \alpha, z) = \left\| \mathbf{S} \begin{bmatrix} x_{\text{pred}} \\ \dot{x}_{\text{pred}} \\ \ddot{x}_{\text{pred}} \end{bmatrix} - \mathbf{y}_m \right\|_2^2 \quad (\text{Case 1}) \quad (8a)$$

and

$$\mathcal{L}(\mathbf{y}_m; \theta, z) = \left\| \mathbf{S} \begin{bmatrix} x_{\text{pred}} \\ \dot{x}_{\text{pred}} \\ \ddot{x}_{\text{pred}} \end{bmatrix} - \mathbf{y}_m \right\|_2^2 \quad (\text{Case 2}) \quad (8b)$$

where the selection matrix $\mathbf{S} \in \mathbb{R}^{d \times 3}$ selects specific quantities from data $[x_{\text{pred}}, \dot{x}_{\text{pred}}, \ddot{x}_{\text{pred}}]^T \in \mathbb{R}^{3 \times N}$, compared with available measurements $\mathbf{y}_m \in \mathbb{R}^{d \times N}$; $d = 1, 2$, or 3 is the number of measured quantities, and N is the total number of time steps. After convergence, this process yields the predicted system responses x_{pred} , \dot{x}_{pred} , and \ddot{x}_{pred} , also with predicted internal variables z_{pred} and \dot{z}_{pred} .

Through this step, the internal hysteretic variable is learned directly from the measurements, addressing one of the central difficulties in hysteresis modeling. Importantly, this process avoids restrictive assumptions, such as prescribing a specific functional form for the hysteretic link equation (g_ϕ) or relying on strongly constrained structural priors, and provides essential data-driven guidance for the subsequent *Equation discovery*, where SR is employed to recover explicit governing equations.

3.3. Equation discovery

The final step of the framework is dedicated to extract interpretable governing equations. For the hysteretic link equation (g_ϕ), as illustrated in Figure 2, symbolic regression (SR) is applied to the learned trajectories of \dot{x}_{pred} , z_{pred} , and \dot{z}_{pred} to search for mathematical expressions $\dot{z} = g_\phi(\dot{x}, z)$, and this can be written as $\text{SR}(\dot{z}_{\text{pred}}, \dot{x}_{\text{pred}}, z_{\text{pred}})$. For dynamic motion equation (f_θ), in *Case 1: Hysteresis Discovery* case, with known equation structure and the estimated values of m, c, k, α , the discovered dynamic motion equation is expressed as $f_\theta = (u - c\dot{x} - kx - \alpha z)/m$; In *Case 2: Full Equation Discovery*, using the same SR method, we can obtain the discovered dynamic motion equation $\ddot{x} = f_\theta(x, \dot{x}, z, u)$, and this can be written as $\text{SR}(\ddot{x}_{\text{pred}}, x_{\text{pred}}, \dot{x}_{\text{pred}}, z_{\text{pred}}, u)$.

A key advantage of SR lies in its flexibility. Unlike approaches such as SINDy that rely on a predefined functional library, SR enables customisation of the search space by incorporating possible operators (e.g., absolute value and exponential) and explicit control over expression complexity. In particular, SR allows the specification of operator forms without fixing their exact exponents or coefficients – for example, one can include $|\cdot|^n$ with n treated as a free constant to be learned. This stands in contrast to SINDy, which requires enumerating many such candidate terms in the predefined library, making it impractical or unfriendly when n is non-integer. Our subsequent experiments will further illustrate this difference. This adaptability mitigates overfitting, promotes interpretability, and facilitates the recovery of compact, physically plausible differential equations that reliably describe the system dynamics.

4. Experiments

To evaluate the effectiveness and robustness of the proposed framework, we apply the framework to a series of experiments on representative hysteretic systems. These experiments aim to assess both predictive accuracy and generalization ability under varying excitation types, noise conditions and initial conditions. For the noise conditions part, robustness with respect to measurement uncertainty is examined by adding zero-mean Gaussian white noise to measured data, with signal-to-noise ratio (SNR) defined as:

$$\text{SNR}(dB) = 10 \log_{10} \left(\frac{P_{\text{signal}}}{P_{\text{noise}}} \right), \quad (9)$$

where P_{signal} and P_{noise} denote the average power of the clean signal and the added noise, respectively. To better demonstrate the performance of the proposed framework, the prediction accuracy is quantified using the normalized root mean square error (NRMSE), defined as:

$$\text{NRMSE}(y_{\text{pred}}, y_{\text{true}}) = \frac{\sqrt{\frac{1}{N} \sum_{i=1}^N (y_{\text{pred},i} - y_{\text{true},i})^2}}{\max\{y_{\text{true}}\} - \min\{y_{\text{true}}\}}, \quad (10)$$

where $y_{\text{true},i}$ and $y_{\text{pred},i}$ denote the i -th observed (ground truth) and predicted values of the target quantity, respectively; N is the total number of samples. The normalization by the range of y_{true} ensures scale-invariant comparison across different datasets or measurement magnitudes.

The subsequent subsections present three case studies of increasing complexity: (i) the Bouc-Wen hysteretic system benchmark, (ii) a complex structure with nonlinear and fractional terms, and (iii) an experimental SDOF yielding structure. Collectively, these experiments provide a comprehensive evaluation of the unified framework across challenging modeling scenarios.

4.1. Bouc-Wen hysteretic system benchmark

The Bouc-Wen hysteretic benchmark, developed by Noël and Schoukens [27], provides a well-established testbed for evaluating nonlinear system identification methods under hysteretic dynamics. The benchmark builds on the Bouc-Wen model of hysteresis [7, 45], which has been extensively used in structural dynamics and control applications [46, 47]. The benchmark data are generated through accurate integration of the Bouc-Wen equations using a Newmark scheme, including estimation data obtained from noisy multisine excitations for model identification, as well as separate fixed test datasets for validation. In particular, two fixed test datasets are provided: (i) a sinesweep excitation with amplitude of 40 N sweeping from 20 - 50 Hz and (ii) a random-phase multisine excitation covering the 5 - 150 Hz frequency band [27]. These datasets are widely adopted in the system identification community for assessing generalization capabilities of nonlinear models.

In our experiments, the sinesweep dataset is used for training, while the multisine dataset is reserved for testing. This configuration evaluates the ability of the proposed framework to generalize across different excitation types. The goal is not only to capture the nonlinear hysteretic dynamics present in the training data but also to validate robustness and predictive accuracy under unseen forcing conditions.

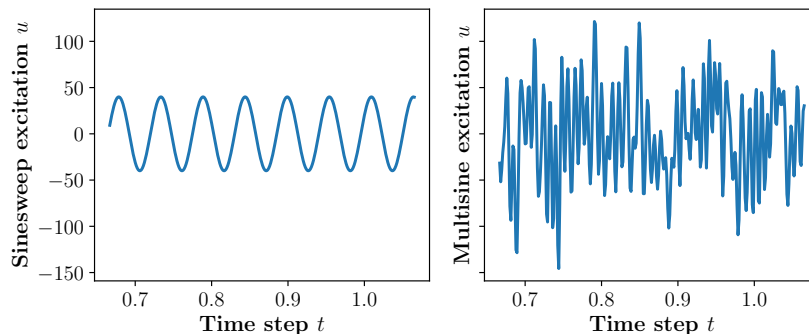


Figure 3: Different types of external excitation of benchmark data. The sinesweep signal (left) is used as the training input, while the multisine signal (right) serves as the testing input.

The Bouc-Wen hysteretic system can be described by a SDOF nonlinear mass-spring-damper oscillator, where the restoring force includes both elastic and hysteretic components. Following the benchmark description in [27], the dynamics are governed by the coupled differential equations:

$$\begin{cases} m\ddot{x}(t) + c\dot{x}(t) + kx(t) + \alpha z(t) = u(t), \\ \dot{z}(t) = A\dot{x}(t) - \beta|\dot{x}(t)||z(t)|^{n-1}z(t) - \gamma\dot{x}(t)|z(t)|^n, \end{cases} \quad (11)$$

where $x(t)$ is the displacement response, $u(t)$ is the external excitation, and $z(t)$ is the internal hysteretic variable. The parameters m , c , and k denote the mass, damping, and linear stiffness, respectively, while α , A , β , γ , and n control the amplitude, shape, and smoothness of the hysteresis loop. For the benchmark configuration, the parameters are set to $m = 2.0$, $c = 10.0$, $k = 50000.0$, $\alpha = 1.0$, $A = 50000.0$, $\beta = 800.0$, $\gamma = -1100.0$ and $n = 1.0$.

As the first benchmark case, Figure 3 illustrates the two external excitations employed for training and testing: a sinesweep signal and a multisine signal. In addition, we further consider noisy scenarios by adding Gaussian noise with signal-to-noise ratios of 30 dB, 25 dB, and 20 dB, corresponding to low, medium, and high noise levels, respectively.

In this benchmark example, we assume to know the structure of the dynamics motion equation, thus it is a problem of *Hysteresis Discovery*, defined in Figure 1. Based on this set-up, Figure 4 shows the hysteresis loops learned by the proposed framework, in terms of three different representations. It can be observed that, even in the presence of strong noise, the proposed model successfully captures nonlinear memory-dependent hysteretic behaviors.

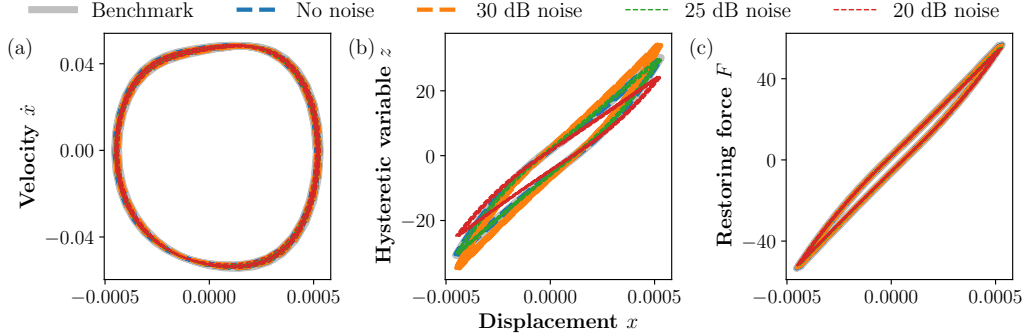


Figure 4: Hysteresis loops of benchmark data. (a) $x - \dot{x}$ hysteresis loop. (b) $x - z$ hysteresis loop. (c) $x - F(F = kx + \alpha z)$ hysteresis loop.

We define two different types of testing cases. In Testing 1, the external excitation is the same as in Training, but the data are taken from a time interval beyond the Training window. In Testing 2, by contrast, a different external excitation is applied, providing an out-of-distribution scenario relative to Training.

For a quantitative evaluation, Tables 1 and 2 report the performance in terms of discovered equations and NRMSE at different noise levels, respectively. The results show that the proposed framework consistently achieves an accurate reconstruction of explicit governing equations, with the responses reproduced from the discovered explicit equations exhibiting low NRMSE values.

Table 1: Discovered equations results of benchmark data (t is omitted for brevity). The true equations are $2\ddot{x} + 10\dot{x} + 50000x + z = u$ and $\dot{z} = 50000\dot{x} - 800|\dot{x}|z + 1100\dot{x}|z|$.

Noise	Discovered equations
Noise-free	$1.9998\ddot{x} + 10.0231\dot{x} + 49893.8617x + 1.0110z = u$ $\dot{z} = 49633.1496\dot{x} - 779.1857 \dot{x} z + 1049.3318\dot{x} z $
30dB	$1.9552\ddot{x} + 10.0124\dot{x} + 49063.4476x + 0.8907z = u$ $\dot{z} = 60143.4371\dot{x} - 811.8583 \dot{x} z + 811.8583\dot{x} z $
25dB	$1.8623\ddot{x} + 10.2269\dot{x} + 47507.9528x + 1.0210z = u$ $\dot{z} = 50858.0627\dot{x} - 734.82275 \dot{x} z + 922.7398\dot{x} z $
20dB	$1.7976\ddot{x} + 12.8240\dot{x} + 46127.6819x + 1.2557z = u$ $\dot{z} = 43574.2517\dot{x} - 727.0708 \dot{x} z + 727.0708\dot{x} z $

Table 2: NRMSE results of benchmark data.

Noise	Responses	Training NRMSE	Testing 1 NRMSE	Testing 2 NRMSE
Noise-free	Displacement x	0.15%	0.13%	0.93%
	Velocity \dot{x}	0.44%	0.49%	1.06%
30 dB	Displacement x	0.85%	0.78%	0.67%
	Velocity \dot{x}	1.29%	1.13%	0.96%
25 dB	Displacement x	1.86%	1.43%	3.24%
	Velocity \dot{x}	2.55%	1.88%	3.41%
20 dB	Displacement x	2.41%	1.64%	3.30%
	Velocity \dot{x}	3.08%	2.15%	3.37%

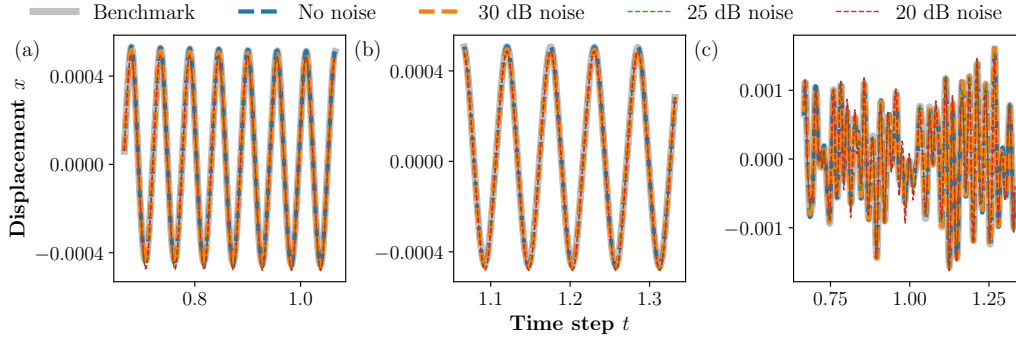


Figure 5: Displacement results of benchmark data. (a) Training results. (b) Testing 1 (same excitation) results. (c) Testing 2 (different excitation) results.

To further assess the validity of the discovered models, Figures 5 and 6 compare the displacement and velocity responses obtained by numerically solving the discovered governing equations against the ground-truth responses, respectively. The discovered dynamic equations are numerically solved to obtain the solution trajectories, which are then compared with the benchmark data. This procedure more directly highlights the effectiveness of equation discovery. This benchmark experiment demonstrates that the unified three-step framework is capable of reliably identifying hysteretic dynamics, even under noisy conditions. These findings validate the effectiveness of the proposed methodology for equation discovery and dynamic prediction of nonlinear hysteretic systems.

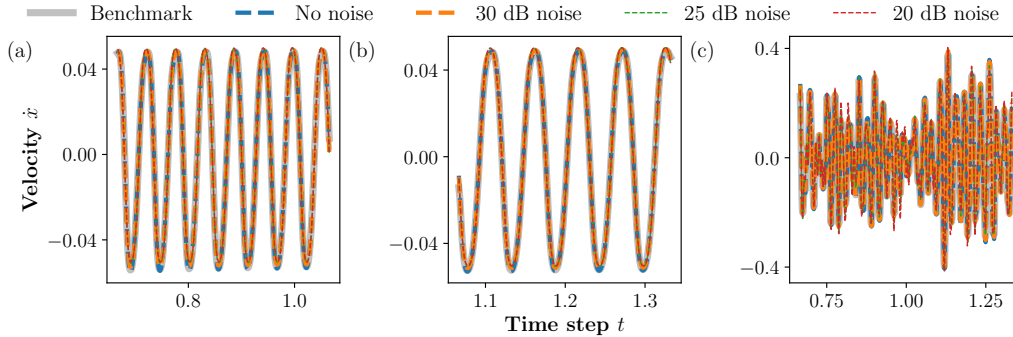


Figure 6: Velocity results of benchmark data. (a) Training results. (b) Testing 1 (same excitation) results. (c) Testing 2 (different excitation) results.

4.2. A complex structure with high-order nonlinear and fractional terms

The second experiment considers a more complex hysteretic system to further evaluate the flexibility of the proposed framework. In this case, the restoring force incorporates a cubic nonlinearity in the displacement response, and the hysteretic evolution equation involves a fractional exponent n , thereby introducing additional challenges compared to the standard Bouc-Wen formulation. The governing equations are given by:

$$\begin{cases} m\ddot{x}(t) + c\dot{x}(t) + kx(t)^3 + \alpha z(t) = u(t), \\ \dot{z}(t) = A\dot{x}(t) - \beta|\dot{x}(t)||z(t)|^{n-1}z(t) - \gamma\dot{x}(t)|z(t)|^n, \end{cases} \quad (12)$$

with system parameters $m = 1.0$, $c = 0.8$, $k = 0.5$, $\alpha = 1.0$, $A = 4.0$, $\beta = 5.0$, and $\gamma = -4.0$. Unlike the benchmark case, here we let $n = 1.5$ (fractional), which modifies the smoothness and sharpness of the hysteretic transition and better reflects diverse hysteretic behaviors.

To test the generalizability, the training and testing datasets are generated under different initial conditions. This experiment highlights the unified nature of the framework, as it remains applicable even when the underlying system exhibits higher-order nonlinearities and non-integer hysteretic exponents.

In this experiment, we consider two challenging cases as in Figure 1 and 2, namely *Hysteresis Discovery* and *Full Equation Discovery*, which differ in whether the dynamics motion equation (f_θ) structure is assumed to be known (the structure of the hysteretic link equation (g_ϕ) is assumed to be unknown in both cases). This comparison enables us to examine the impact

of prior structural knowledge on equation discovery for complex hysteretic systems. In this experiment, five different initial conditions are used for training, while an additional unseen initial condition is used for testing to evaluate the generalizability of the proposed framework. The external excitation is defined as $u(t) = \sin(2t)$, representing a smooth periodic input suitable for dynamic identification. The sampling frequency is set to $f_s = 100$ Hz, and the total simulation duration is $T = 6s$. Such a setup allows for a comprehensive assessment of the model’s robustness under varying initial states while maintaining consistent excitation characteristics.

Figure 7 shows the hysteresis loops learned by the solver-based internal variable learning module. Both configurations can capture qualitative hysteretic behavior, yet the *Hysteresis Discovery* model clearly achieves better accuracy in reconstructing the loop dynamics. Table 3 lists the explicit forms of the discovered equations, and Table 4 reports the NRMSE results. Figures 8 and 9 compare the displacement, velocity, and acceleration responses obtained by solving the discovered equations, compared with the corresponding ground-truth responses in the training and testing datasets, respectively.

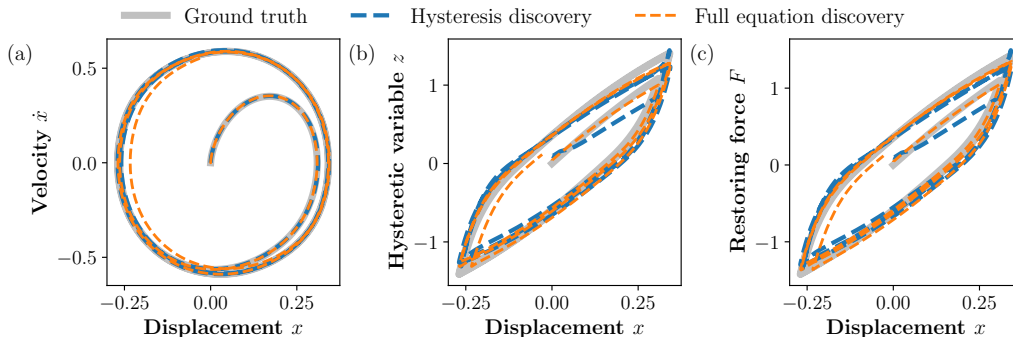


Figure 7: Hysteresis loops of complex structure data. (a) $x - \dot{x}$ hysteresis loop. (b) $x - z$ hysteresis loop. (c) $x - F (F = kx^3 + \alpha z)$ hysteresis loop.

From these results, it is evident that the proposed framework consistently outperforms SINDy, achieving lower errors and more faithful recovery of the governing equations. For SINDy, the pre-defined library was designed to be as consistent as possible with our method: the dynamics motion equation is assumed to be a linear combination of x , \dot{x} , z , and u , while the hysteretic link equation is constrained to contain absolute values and their integer powers (from 1 to 5), to provide SINDy with sufficient expressive capacity for cap-

turing nonlinear hysteretic behaviors. However, unlike SR, SINDy cannot flexibly capture fractional exponents.

In particular, both *Hysteresis Discovery* and *Full Equation Discovery* can successfully recover expressions with fractional exponents in Eq.(12), which is generally beyond the capability of library-based approaches such as SINDy. By contrast, the *Full Equation Discovery* setting—where both the dynamics motion equation and the hysteretic link equation are unknown—yields slightly lower accuracy than *Hysteresis Discovery*. In practice, it is suggested that incorporating some prior knowledge helps improve accuracy and equation discovery performance.

Table 3: Discovered equations results of complex structure data (t is omitted for brevity). The true equations are $1.0\ddot{x}+0.8\dot{x}+0.5x^3+1.0z = u$ and $\dot{z} = 4.0\dot{x}-5.0|\dot{x}||z|^{0.5}z+4.0\dot{x}|z|^{1.5}$. SINDy fails to recover the fractional order terms and instead introduces spurious integer order terms to compensate.

Type and method	Discovered equations
<i>Hysteresis Discovery</i> (Ours)	$0.9388\ddot{x} + 0.7934\dot{x} + 0.5366x^3 + 1.0320z = u$ $\dot{z} = 4.0633\dot{x} - 4.8310 \dot{x} z ^{0.5486}z + 3.8942\dot{x} z ^{1.5486}$
<i>Hysteresis Discovery</i> (SINDy)	$\ddot{x} + 0.8445\dot{x} + 0.5679x^3 + 1.0992z = 1.0649u$ $\dot{z} = -6.80922 \dot{x} z z + 5.00018 \dot{x} z ^2z + 4.98652\dot{x} z ^2 + 3.73699\dot{x}$
<i>Full Equation Discovery</i> (Ours)	$\ddot{x} + 0.7689\dot{x} + 0.4573x^3 + 1.0423z = 0.9503u$ $\dot{z} = 4.0543\dot{x} - 5.1348 \dot{x} z ^{0.6225}z + 3.8224\dot{x} z ^{1.6225}$
<i>Full Equation Discovery</i> (SINDy)	$\ddot{x} + 0.7490\dot{x} + 0.5833x^3 + 1.2145z = 0.8992u$ $\dot{z} = -12.704 \dot{x} z z + 6.118 \dot{x} z ^2z + 2.941\dot{x} z ^2 - 0.873\dot{x}$

Table 4: NRMSE results of complex structure data.

Type	Responses	Training NRMSE (Ours)	Testing NRMSE (Ours)	Training NRMSE (SINDy)	Testing NRMSE (SINDy)
<i>Hysteresis discovery</i>	Displacement x	4.21%	3.84%	25.42%	36.87%
	Velocity \dot{x}	3.91%	4.01%	24.79%	39.50%
	Acceleration \ddot{x}	3.86%	3.88%	25.70%	40.67%
<i>Full equation discovery</i>	Displacement x	5.28%	4.57%	25.73%	37.76%
	Velocity \dot{x}	4.56%	4.25%	26.56%	32.43%
	Acceleration \ddot{x}	4.86%	4.31%	23.00%	36.15%

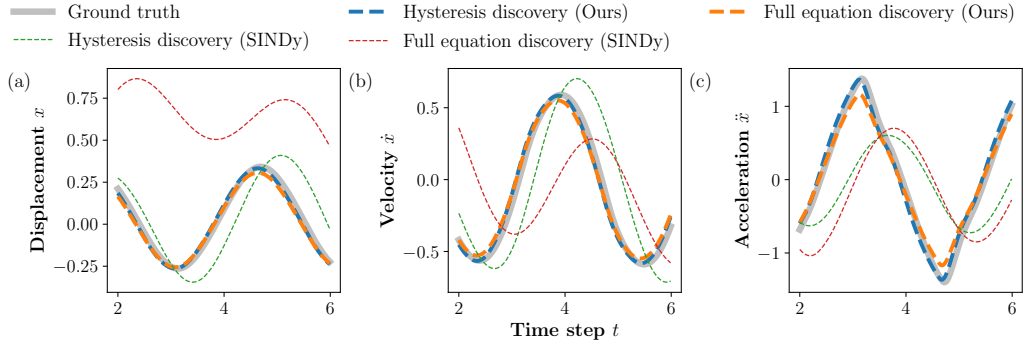


Figure 8: Training results of complex structure data. (a) Displacement results. (b) Velocity results. (c) Acceleration results.

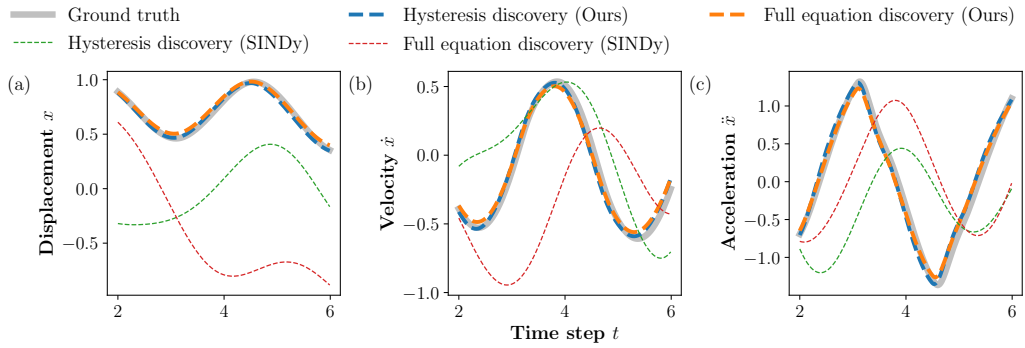


Figure 9: Testing results of complex structure data. (a) Displacement results. (b) Velocity results. (c) Acceleration results.

4.3. An experimental SDOF yielding structure

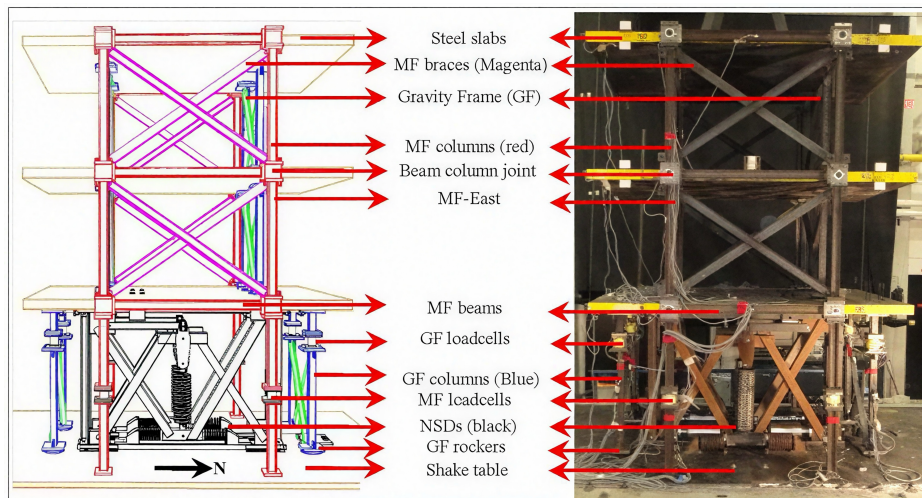


Figure 10: Shaking table test of a braced 3-story structure (equivalent to a SDOF system), with a negative stiffness device (NSD) installed on the first floor [26].

In this experiment, a shear-type SDOF yielding structure excited by shake-table motions is implemented to investigate the proposed method. The experimental setup of the braced 3-story structure (equivalent to a SDOF system), with and without a negative stiffness device (NSD) [48, 49] is illustrated in Figure 10 [26, 50, 51], where the NSD is installed on the first floor to alter hysteretic behaviors.

We adopt the governing equation structure $m\ddot{x}(t) + c\dot{x}(t) + kx(t) + \alpha z(t) = -mu(t)$, where $x(t)$ is the displacement, $\dot{x}(t)$ and $\ddot{x}(t)$ are its velocity and acceleration, $u(t)$ is the measured base acceleration, and $z(t)$ is the hysteretic internal variable. This setup belongs to the *hysteresis discovery* type, in which the structure of the equation of motion is predefined (which needs to identify unknown system parameters), and the nonlinear hysteretic link equation is assumed to be unknown.

We reuse the real shake table experiment from [26], and study the structure in two scenarios: (i) *without* an NSD and (ii) *with* an NSD installed on the first floor. Following the setup in [26], we use the measured displacement $x(t)$, the computed velocity $\dot{x}(t)$ (via differentiation and smoothing), the measured acceleration $\ddot{x}(t)$, and the shake-table excitation $u(t)$ as inputs to our framework. For the *without NSD* case, a type-I 60% scaled Pacoima

earthquake is used for training, and a reversed type-II 60% Pacoima record for testing. For the *with NSD* case, the training signal concatenates 43% and 65% scaled Pacoima segments, while the testing input is a 55% scaled Sylmar record (see Figs. 23–25 of [26] for details).

For the *without NSD* case, the hysteresis loop in the x – \dot{x} plane is presented in Figure 11(a). The discovered evolution law reduces to rate-dominated form $\dot{z}(t) = 2.1847\dot{x}(t)$, together with the dynamics motion equation $22.2798\ddot{x}(t) + 18.4829\dot{x}(t) + 1571.7874x(t) + 1572.5618z(t) = -22.2798u(t)$, which in nature is a linear system. This reflects that our proposed framework is capable of automatically discovering a linear equation if the system comes without evident nonlinearity or hysteresis. Figures 12 and 13 show that the model closely matches the training and testing responses in terms of displacement, velocity, and acceleration. Table 5 provides quantitative results. The small NRMSEs confirm that the framework achieves accurate and robust identification when the hysteresis is mild and rate-dominated.

For the *with NSD* case, the hysteresis loops become much wider and exhibit obvious pinching and asymmetry (Figure 11(b)). Accordingly, the learned $\dot{z}(t)$ includes higher-order and mixed-magnitude terms of $x(t)$, $\dot{x}(t)$, and $z(t)$. The predicted hysteretic link equation is $\dot{z}(t) = 4.8586\dot{x}(t) + 1.6412x^2|\dot{x}(t)| + 1.8160\dot{x}(t)|\dot{x}(t)|z(t) - 1.8174\dot{x}(t)|z(t)| + 1.7648z(t)|z(t)|$ with the dynamics motion equation $22.2798\ddot{x}(t) + 44.7281\dot{x}(t) + 2099.6526x(t) + 2108.1516z(t) = -22.2798u(t)$. As shown in Figures 14 and 15, the training responses are well captured, but testing displacement exhibits larger deviations. Table 5 confirms this: the displacement error rises to 14.11% in the testing set, while velocity and acceleration remain within 6%. This indicates that the NSD introduces stronger nonlinear hysteresis, which requires a richer \dot{z} structure and leads to a larger generalization gap. In other words, the model still succeeds in capturing the main nonlinear patterns, but the predictive accuracy is more sensitive to unseen excitations.

From all these results, it can be concluded that the proposed framework is capable of both equation discovery and dynamic prediction in real experimental data. For the relatively simple *without NSD* case, it achieves concise and highly accurate identification, while for the more challenging *with NSD* case, it still provides interpretable governing equations and meaningful forward predictions, albeit with a higher generalization error. In future work, these limitations may be further addressed by extending the framework toward more complex hysteretic systems and improving its generalization to a wider range of nonlinear dynamical problems.

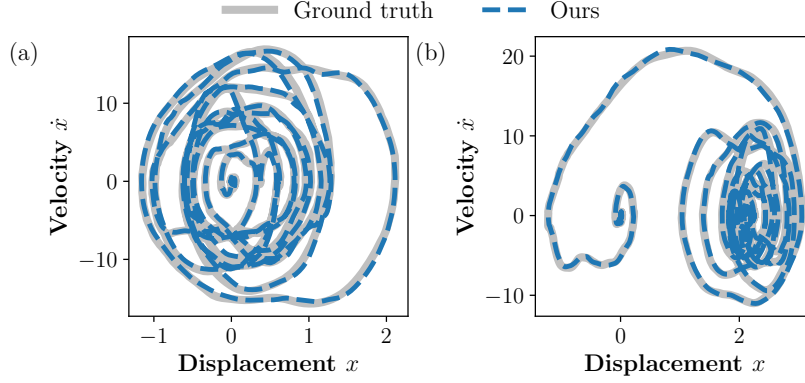


Figure 11: $x - \dot{x}$ hysteresis loops of yielding structure. (a) Without NSD. (b) With NSD.

Table 5: NRMSE results of yielding structure data.

Scenarios	Responses	Training NRMSE (Ours)	Testing NRMSE (Ours)	Training NRMSE (Sparse [26])	Testing NRMSE (Sparse [26])
Without NSD	Displacement x	3.23%	2.99%	10.73%	2.90%
	Velocity \dot{x}	2.57%	2.89%	4.47%	2.92%
	Acceleration \ddot{x}	1.45%	2.14%	4.42%	2.70%
With NSD	Displacement x	4.12%	14.11%	6.57%	13.85%
	Velocity \dot{x}	4.49%	5.60%	4.56%	5.62%
	Acceleration \ddot{x}	5.96%	4.86%	5.71%	6.26%

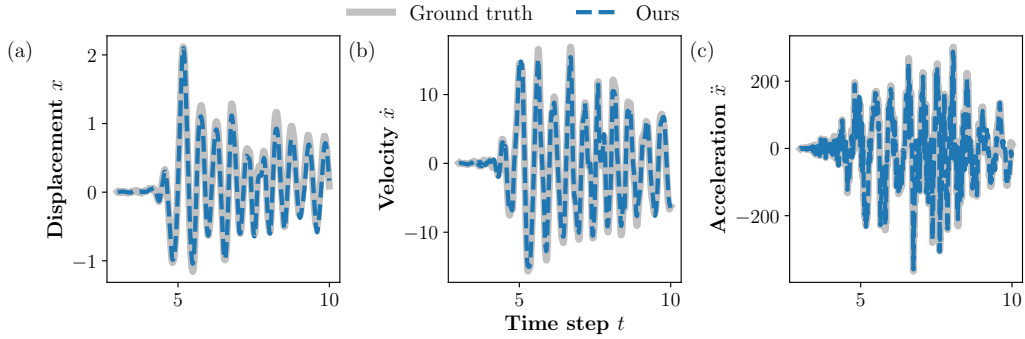


Figure 12: Training results of yielding structure data without NSD. (a) Displacement results. (b) Velocity results. (c) Acceleration results.

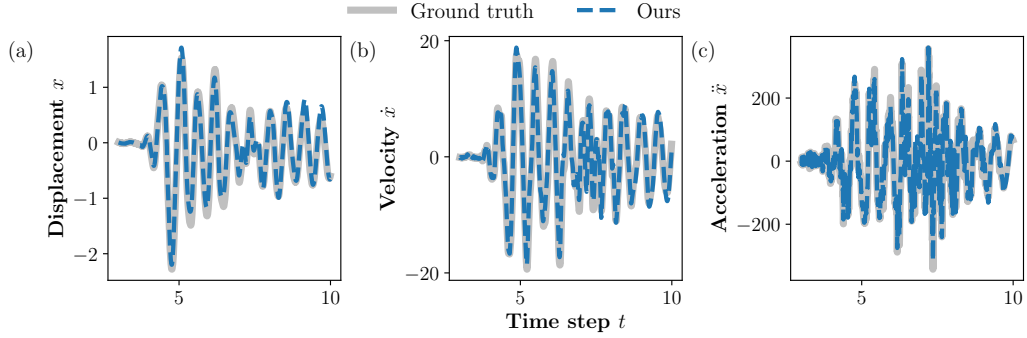


Figure 13: Testing results of yielding structure data without NSD. (a) Displacement results. (b) Velocity results. (c) Acceleration results.

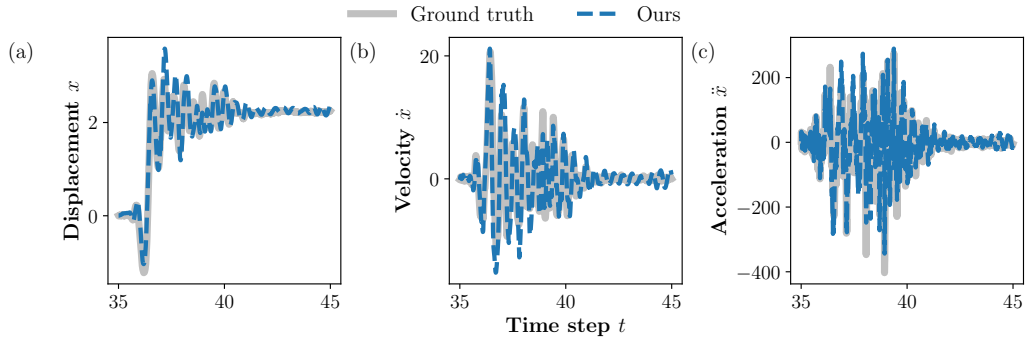


Figure 14: Training results of yielding structure data with NSD. (a) Displacement results. (b) Velocity results. (c) Acceleration results.

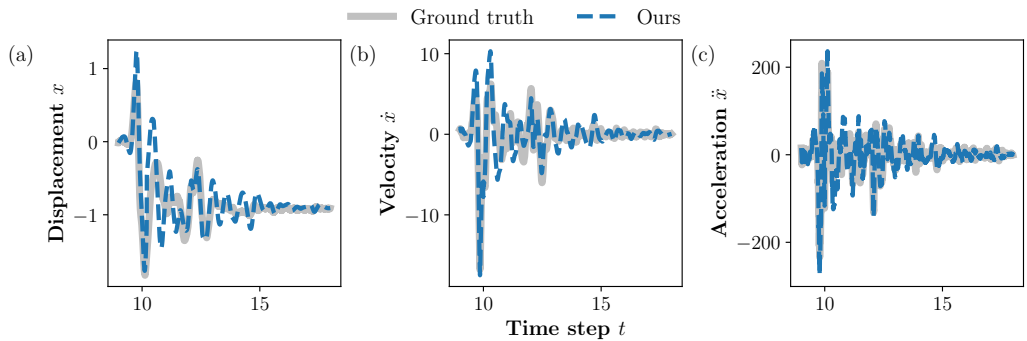


Figure 15: Testing results of yielding structure data with NSD. (a) Displacement results. (b) Velocity results. (c) Acceleration results.

5. Conclusion

This research presented a unified framework for equation discovery and dynamic prediction of hysteretic systems, with a proposed solver-based internal variable learning scheme that addresses one of the key challenges in hysteresis modeling – the difficulty of inferring internal variables. We summarize existing work on equation discovery for hysteretic systems and categorize them according to the level of assumed knowledge available. The proposed unified framework in our work is capable of addressing two major challenges of hysteretic systems across various scenarios: the learning of unobservable internal variables and the discovery of governing equations with complex nonlinear expressions. The effectiveness of the framework is validated through three representative case studies. On the Bouc-Wen benchmark, it accurately recovers the governing equations even in the presence of noise, confirming its robustness and reliability. For a more complex nonlinear structure with cubic stiffness and fractional hysteretic exponents, the framework successfully achieves superior accuracy and interpretability compared with library-based methods such as SINDy. In the real shake-table experiment of a yielding structure, the framework reveals concise rate-dominated dynamics without NSD and more complex nonlinear hysteresis behavior with NSD, achieving stable predictions.

This research not only provides insights into equation discovery and dynamic prediction of hysteretic systems but also demonstrates the potential of the proposed framework for broader applications in nonlinear dynamical systems, including those with or without internal variables. Its flexibility and interpretability make it applicable to various domains such as structural dynamics, material modeling, and control system identification, where nonlinear and memory-dependent behaviors are common. Future work will focus on enhancing the efficiency and scalability of the framework, improving its ability to handle higher-dimensional systems, and exploring probabilistic or hybrid modeling strategies to further extend its applicability to real-world engineering and scientific problems.

Acknowledgments

The authors would like to express their sincere gratitude to Prof. Satish Nagarajaiah at Rice University for generously sharing the experimental data of SDOF yielding structure that made this research possible. The authors wish to express their gratitude for the financial support received from Guangdong Provincial Fund - Special Innovation Project (2024KTSCX038); Research Grants Council of Hong Kong through the Research Impact Fund (R5006-23); the Guangdong Provincial Key Lab of Integrated Communication, Sensing and Computation for Ubiquitous Internet of Things (No. 2023B1212010007).

References

- [1] D. C. Jiles, D. L. Atherton, Theory of ferromagnetic hysteresis, *Journal of magnetism and magnetic materials* 61 (1-2) (1986) 48–60.
- [2] M. Al Janaideh, C.-Y. Su, S. Rakehja, Modeling hysteresis of smart actuators, in: 2008 5th International Symposium on Mechatronics and Its Applications, IEEE, 2008, pp. 1–4.
- [3] G. Bertotti, *Hysteresis in magnetism: for physicists, materials scientists, and engineers*, Academic press, 1998.
- [4] E. Ko, I. Kimura, P. Clark, I. Aiken, K. Kasai, Design procedures for buildings incorporating hysteretic damping devices, in: *Proceedings of the 68th Annual Convention SEAOC*, Santa Barbara, CA, USA, Vol. 30, 1999.
- [5] A. Dominguez, R. Sedaghati, I. Stiharu, Modelling the hysteresis phenomenon of magnetorheological dampers, *Smart Materials and Structures* 13 (6) (2004) 1351.
- [6] J. Ortín, L. Delaey, Hysteresis in shape-memory alloys, *International Journal of Non-Linear Mechanics* 37 (8) (2002) 1275–1281.
- [7] Y.-K. Wen, Method for random vibration of hysteretic systems, *Journal of the engineering mechanics division* 102 (2) (1976) 249–263.

- [8] C. Visone, Hysteresis modelling and compensation for smart sensors and actuators, in: *Journal of Physics: Conference Series*, Vol. 138, IOP Publishing, 2008, p. 012028.
- [9] E. N. Chatzi, A. W. Smyth, S. F. Masri, Experimental application of on-line parametric identification for nonlinear hysteretic systems with model uncertainty, *Structural Safety* 32 (5) (2010) 326–337.
- [10] A. Chandra, B. Daniels, M. Curti, K. Tiels, E. A. Lomonova, D. M. Tartakovsky, Discovery of sparse hysteresis models for piezoelectric materials, *Applied Physics Letters* 122 (21) (2023).
- [11] Y. Liu, K. P. Kelley, R. K. Vasudevan, H. Funakubo, M. A. Ziatdinov, S. V. Kalinin, Experimental discovery of structure–property relationships in ferroelectric materials via active learning, *Nature Machine Intelligence* 4 (4) (2022) 341–350.
- [12] K. Vlachas, K. Agathos, K. E. Tatsis, A. R. Brink, E. Chatzi, Two-story frame with bouc-wen hysteretic links as a multi-degree of freedom nonlinear response simulator, in: *5th Workshop on Nonlinear System Identification Benchmarks*, ETH Zurich, 2021.
- [13] I. D. Mayergoyz, *Mathematical models of hysteresis and their applications*, Academic press, 2003.
- [14] J. Oh, D. S. Bernstein, Semilinear duhem model for rate-independent and rate-dependent hysteresis, *IEEE Transactions on Automatic Control* 50 (5) (2005) 631–645.
- [15] A. Visintin, *Differential models of hysteresis*, Vol. 111, Springer Science & Business Media, 2013.
- [16] S. H. Rudy, S. L. Brunton, J. L. Proctor, J. N. Kutz, Data-driven discovery of partial differential equations, *Science advances* 3 (4) (2017) e1602614.
- [17] B. Chen, C. Zhang, J. Zhang, Y. Wang, Adaptive physics-informed system modeling with control for nonlinear structural system estimation, *Computer Methods in Applied Mechanics and Engineering* 447 (2025) 118330.

- [18] M. Haywood-Alexander, W. Liu, K. Bacsa, Z. Lai, E. Chatzi, Discussing the spectrum of physics-enhanced machine learning: a survey on structural mechanics applications, *Data-Centric Engineering* 5 (2024) e30.
- [19] L. Yi, S. Yang, Y. Cui, Z. Lai, Transforming physics-informed machine learning to convex optimization, *Engineering Applications of Artificial Intelligence* 161 (2025) 112149.
- [20] S. Yang, C. Song, Z. Lai, W. Wang, KP-PINNs: Kernel packet accelerated physics informed neural networks, in: *Proceedings of the Thirty-Fourth International Joint Conference on Artificial Intelligence, IJCAI-25, 2025*, pp. 7904–7912.
- [21] L. Yan, H. Cai, Q. Wang, L. Chen, C. Li, G. Hu, Deep reinforcement learning-based active flow control for a tall building, *Physics of Fluids* 37 (4) (2025).
- [22] S. L. Brunton, J. L. Proctor, J. N. Kutz, Discovering governing equations from data by sparse identification of nonlinear dynamical systems, *Proceedings of the national academy of sciences* 113 (15) (2016) 3932–3937.
- [23] K. P. Champion, S. L. Brunton, J. N. Kutz, Discovery of nonlinear multiscale systems: Sampling strategies and embeddings, *SIAM Journal on Applied Dynamical Systems* 18 (1) (2019) 312–333.
- [24] Z. Chen, Y. Liu, H. Sun, Physics-informed learning of governing equations from scarce data, *Nature communications* 12 (1) (2021) 6136.
- [25] K. Kaheman, J. N. Kutz, S. L. Brunton, Sindy-pi: a robust algorithm for parallel implicit sparse identification of nonlinear dynamics, *Proceedings of the Royal Society A* 476 (2242) (2020) 20200279.
- [26] Z. Lai, S. Nagarajaiah, Sparse structural system identification method for nonlinear dynamic systems with hysteresis/inelastic behavior, *Mechanical Systems and Signal Processing* 117 (2019) 813–842.
- [27] J.-P. Noel, M. Schoukens, Hysteretic benchmark with a dynamic nonlinearity, in: *Workshop on nonlinear system identification benchmarks, 2016*, pp. 7–14.

- [28] A. Bolourchi, S. F. Masri, O. J. Aldraihem, Studies into computational intelligence and evolutionary approaches for model-free identification of hysteretic systems, *Computer-Aided Civil and Infrastructure Engineering* 30 (5) (2015) 330–346.
- [29] T. Wang, M. Noori, G. Wang, Z. Wu, Symbolic deep learning-based method for modeling complex rate-independent hysteresis, *Computers & Structures* 311 (2025) 107702.
- [30] W. Liu, K. Bacsá, L. C. Tang, E. Chatzi, Structured kolmogorov-arnold neural odes for interpretable learning and symbolic discovery of nonlinear dynamics, *arXiv preprint arXiv:2506.18339* (2025).
- [31] M. Lin, C. Cheng, G. Zhang, B. Zhao, Z. Peng, G. Meng, Identification of bouc-wen hysteretic systems based on a joint optimization approach, *Mechanical Systems and Signal Processing* 180 (2022) 109404.
- [32] K. Worden, J. Hensman, Parameter estimation and model selection for a class of hysteretic systems using bayesian inference, *Mechanical Systems and Signal Processing* 32 (2012) 153–169.
- [33] A. E. Charalampakis, V. K. Koumoussis, Identification of bouc-wen hysteretic systems by a hybrid evolutionary algorithm, *Journal of Sound and Vibration* 314 (3-5) (2008) 571–585.
- [34] J. Qian, X. Sun, J. Xu, L. Cheng, Discovering differential governing equations of hysteresis dynamic systems by data-driven sparse regression method, *Nonlinear Dynamics* 112 (14) (2024) 12137–12157.
- [35] A. Charalampakis, C. Dimou, Identification of bouc-wen hysteretic systems using particle swarm optimization, *Computers & structures* 88 (21-22) (2010) 1197–1205.
- [36] J.-P. Noël, A. F. Esfahani, G. Kerschen, J. Schoukens, A nonlinear state-space approach to hysteresis identification, *Mechanical Systems and Signal Processing* 84 (2017) 171–184.
- [37] N. Novelli, P. Belardinelli, S. Lenci, Identification of hybrid dynamic systems via a sparse regression algorithm, *Nonlinear Dynamics* (2025) 1–24.

- [38] W. Liu, Z. Lai, E. Chatzi, A physics-guided deep learning approach to modeling nonlinear dynamics: A case study of a bouc-wen system, *STRUCTURAL HEALTH MONITORING 2021* (2021).
- [39] W. Liu, Z. Lai, K. Bacsa, E. Chatzi, Physics-guided deep markov models for learning nonlinear dynamical systems with uncertainty, *Mechanical Systems and Signal Processing* 178 (2022) 109276.
- [40] N. M. Newmark, A method of computation for structural dynamics, *Journal of the engineering mechanics division* 85 (3) (1959) 67–94.
- [41] J. C. Butcher, *Numerical methods for ordinary differential equations*, John Wiley & Sons, 2016.
- [42] A. Iserles, *A first course in the numerical analysis of differential equations*, Cambridge university press, 2009.
- [43] M. Cranmer, Interpretable machine learning for science with pysr and symbolicregression. jl, arXiv preprint arXiv:2305.01582 (2023).
- [44] M. Quade, M. Abel, K. Shafi, R. K. Niven, B. R. Noack, Prediction of dynamical systems by symbolic regression, *Physical Review E* 94 (1) (2016) 012214.
- [45] R. Bouc, Forced vibrations of mechanical systems with hysteresis, in: *Proc. of the Fourth Conference on Nonlinear Oscillations*, Prague, 1967, 1967.
- [46] M. Ismail, F. Ikhouane, J. Rodellar, The hysteresis bouc-wen model, a survey, *Archives of computational methods in engineering* 16 (2) (2009) 161–188.
- [47] F. Ikhouane, J. Rodellar, *Systems with hysteresis: analysis, identification and control using the Bouc-Wen model*, John Wiley & Sons, 2007.
- [48] A. A. Sarlis, D. T. R. Pasala, M. Constantinou, A. Reinhorn, S. Nagarajiah, D. Taylor, Negative stiffness device for seismic protection of structures, *Journal of Structural Engineering* 139 (7) (2013) 1124–1133.

- [49] D. Pasala, A. Sarlis, S. Nagarajaiah, A. Reinhorn, M. Constantinou, D. Taylor, Adaptive negative stiffness: new structural modification approach for seismic protection, *Journal of structural Engineering* 139 (7) (2013) 1112–1123.
- [50] D.-T. R. Pasala, A. A. Sarlis, S. Nagarajaiah, A. M. Reinhorn, M. C. Constantinou, D. Taylor, Seismic response control of structures using a novel adaptive passive negative stiffness device, MCEER, 2013.
- [51] N. Attary, M. Symans, S. Nagarajaiah, A. M. Reinhorn, M. C. Constantinou, A. A. Sarlis, D. R. Pasala, D. Taylor, Performance evaluation of negative stiffness devices for seismic response control of bridge structures via experimental shake table tests, *Journal of Earthquake Engineering* 19 (2) (2015) 249–276.